

NASA-CR-204022

PROCEEDINGS REPRINT



SPIE—The International Society for Optical Engineering

*120
10-29-92
10-29-92
10-29-92*

Reprinted from

Space Processing of Materials

4–5 August 1996
Denver, Colorado



Volume 2809

Development of uniform microstructures in immiscible alloys by processing in a low-gravity environment

R.N. Grugel¹ and L.N. Brush²

¹Universities Space Research Association, Marshall Space Flight Center, MS-ES75, Huntsville, AL 35812

²University of Washington, Department of Materials Science and Engineering
Seattle, WA 98195

ABSTRACT

Highly segregated macrostructures tend to develop during processing of hypermonotectic alloys because of the density difference existing between the two liquid phases. The ~4.6 seconds of low-gravity provided by Marshall Space Flight Center's 105 meter drop tube was utilized to minimize density-driven separation and promote uniform microstructures in hypermonotectic Ag-Ni and Ag-Mn alloys. For the Ag-Ni alloys a numerical model was developed to track heat flow and solidification of the bi-metal drop configuration. Results, potential applications, and future work are presented.

INTRODUCTION

Alloy systems exhibiting immiscibility gaps such as Cu-Pb and Al-Pb constitute the basis for a number of technological products, e.g., engine bearings. Unfortunately during solidification processing the inherent, usually large, density difference between the L_I and L_{II} phases promotes rapid separation, coalescence and, subsequently, a highly inhomogeneous structure which compromises the desired material properties. It was envisioned that processing in a microgravity environment would eliminate gravity induced sedimentation and promote a uniform dispersion of L_{II} (eventually S_{II}) in the S_I matrix. Unfortunately, results of experiments conducted in reduced gravity still, for a number of reasons¹⁻³, exhibited highly macrosegregated structures. The intent, therefore, of this work is to demonstrate how a low-gravity environment can be successfully utilized to produce spherical composites in which one phase is uniformly distributed within the other.

EXPERIMENTAL PROCEDURE

Pieces of nickel and manganese were arc-melted to a near spherical shape on the order of 2.5 and 4.5mm in diameter. Figure 1⁴, shows the Ag-Mn phase diagram. Similar in form to Ag-Ni, a high miscibility gap extends over most of the compositional range.

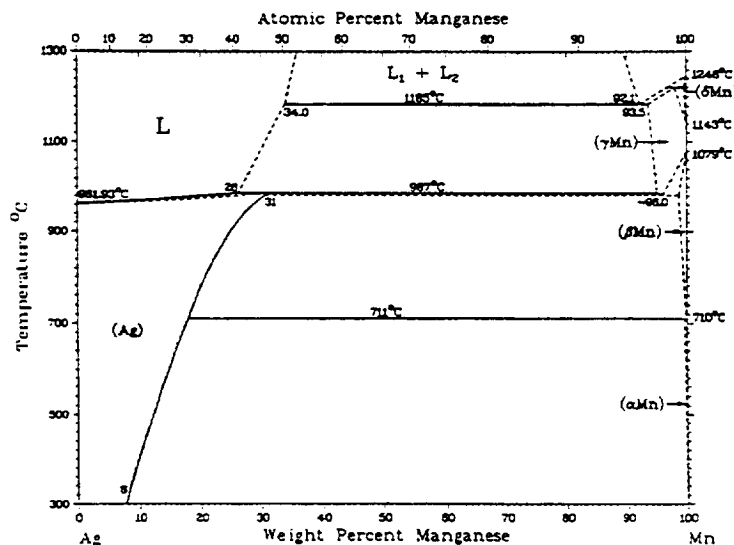


Figure 1: The Ag-Mn phase diagram⁴

The height of the miscibility gap suggests that liquid silver (L_{II}) will preferentially wet both solid (S_I) manganese and nickel⁵. This is confirmed in Figure 2 which shows silver (weighed to eventually surround the core with a 0.5 or 1mm thick layer) that, after melting, wetted the nickel spheres. The overall "bulk" alloy compositions were approximately Ag - 27 or 48 wt pct Ni and Ag - 44 wt pct Mn.



Figure 2: Photograph of the nickel-silver "alloys" prior to processing in the drop tube. Note that the lesser density nickel ($\rho = 8.9\text{gcm}^{-3}$) cores are seen to "float" in the silver ($\rho = 10.5\text{gcm}^{-3}$) pool.

Samples such as those shown above were positioned in the bell jar atop Marshall Space Flight Center's 105 meter drop tube⁶; for these experiments the tube atmosphere consisted of a helium - 6% hydrogen mixture. A given sample was then raised into the electromagnetic (EM) levitator coil and a pyrometer, calibrated to the observed melting of the silver (960.8°C), monitored the sample temperature. Figure 3 shows a typical time-temperature plot, in this case for a Ag-Ni droplet. The horizontal in the trace corresponds to melting of the silver and the sharp drop denotes the sample release temperature. In these experiments the nickel core remained unmelted whereas for the Ag-Mn alloys the temperature could be raised into the two-liquid region.

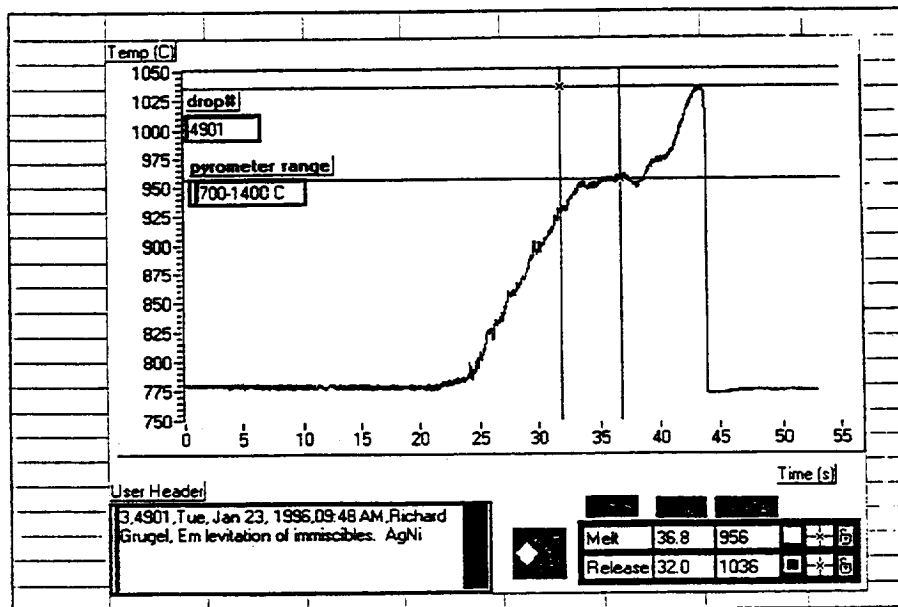


Figure 3: Typical time-temperature plot for the drop tube processed samples

EXPERIMENTAL RESULTS

The retrieved samples were spherical with the few dents a consequence of impacting the bottom. The surface of the nickel-silver sphere was shiny and showed no evidence of the nickel core; the surface of the Ag-Mn sphere was dull. For both alloys the sample weight before and after processing varied by a few thousands of a gram. The processed Ag-Ni spheres were appropriately sectioned⁷ and metallographically prepared. Figure 4 shows an overall spherical sample with impact denoted by the flat. The nickel core is surrounded by silver but not ideally centered.

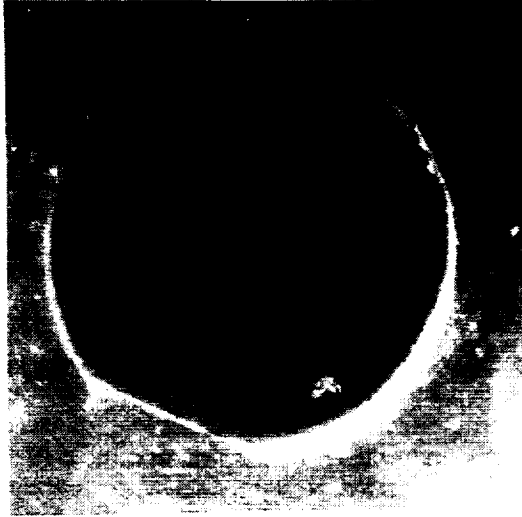
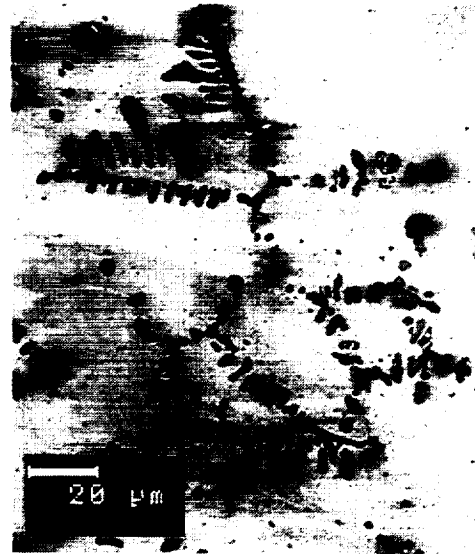


Figure 4: Section through a composite drop noting its overall sphericity and the slight displacement of the ~4mm diameter nickel core; the silver thickness was intended to be 0.5mm.

The processed Ag-Mn spheres were sectioned through their centers and metallographically prepared. The microstructure shown in Figure 5a exhibits an overall uniform distribution of one phase in the other. Higher magnification, Figure 5b, reveals the this phase to consist of fine Mn dendrites.



(5a)



(5b)

Figures 5a and b: Micrographs taken through a section of a processed Ag-Mn droplet.

DISCUSSION

Ideally, the nickel core of the composite drop should be centrally located. An obvious reason is the non-sphericity of the initial nickel droplet. In view of the experimental procedure, and other reasons previously discussed⁷, while liquid silver will wet and form a sphere about the nickel, the shell can never be uniformly thick. Initial modeling of the composite drop's thermal history has also been reported⁷. Briefly, the interfaces between the solid and liquid phases as well as the interface between the two materials and the outer boundary of the composite are assumed spherical. Here a core of material A (nickel) is surrounded by a shell of material B (silver). The radius of material A is designated R_I and the outer boundary radius is given as R_O . R_I and R_O remain fixed throughout time. Material B occupies the region $R_I < r < R_O$. Within materials A and B, one phase (either solid or liquid) or two phases (solid and liquid) are present. In the latter case, the solid-liquid interface within material A has a radius denoted by $R_A(t)$ and the solid-liquid interface within material B has a radius denoted by $R_B(t)$, both of which are functions of time.

The derived bulk heat equations, interfacial conditions and auxiliary boundary conditions, given an initial temperature profile and initial solid-liquid interface positions, can be solved for the positions $R_i(t)$ and the radially varying temperature fields as a function of time. In order to calculate the heat flow and to determine the position of the solid-liquid interface(s) as a function of time for the fully transient problem, a numerical technique is required; work is continuing to this end. Examples of the calculations, using appropriate thermophysical values⁸⁻¹⁰, are shown in Figures 6 and 7.

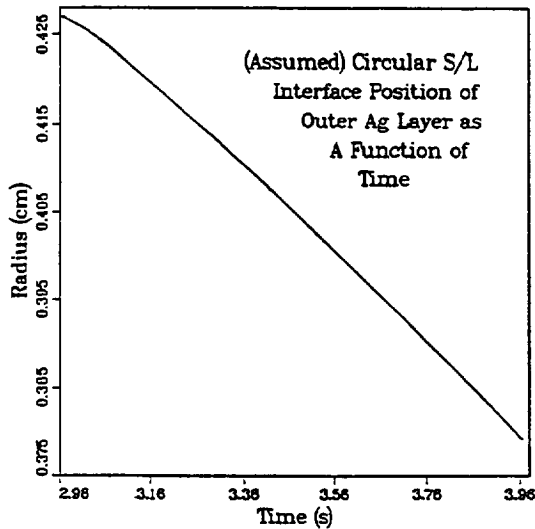


Figure 6: The radial position of the solid-liquid interface as a function of time in the exterior metallic Ag layer. The interface is assumed to maintain a spherical form throughout the solidification event. With an initial condition of $R_I = 0.377\text{cm}$ and $R_O = 0.427\text{cm}$ solidification of the outer shell began at $t = 2.965$ seconds after its release in the drop tube as indicated in the plot. The 0.05 cm thick outer shell froze in a little more than 1 second.

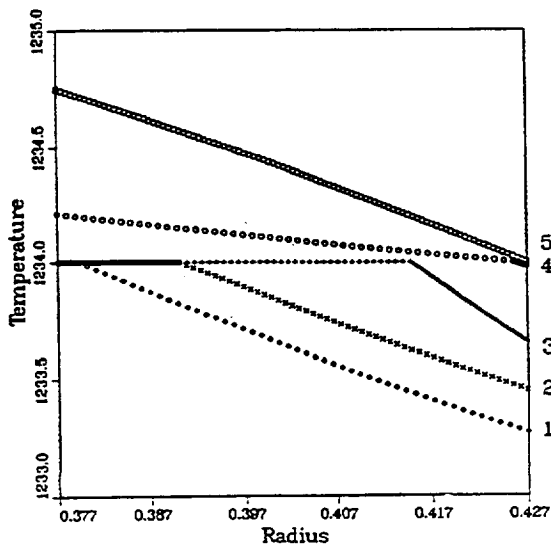


Figure 7: Representative temperature profiles within the Ag layer during the solidification event. The numbers 5 through 1 on the right hand side of the plot correspond to the times 2.96s, 3.015s, 3.265s, 3.765s and 3.965s as given in Figure 6. The outer radial position is 4.27 cm . Solidification was assumed to be initiated uniformly at the outer liquid/gas interface once the temperature had reached the melting point 1234K of the pure, bulk Ag. The curvature effect on the melting temperature of Ag was ignored in this calculation.

As the composite sphere fully solidifies within the 4.6s free-fall time the model appears accurate but is not verified. Work is continuing to expand the model which will then be tested by suitably tailored experiments.

The above treatment is not directly applicable to the experimental results observed with the Ag-Mn alloys. From recorded temperature data and examination of Figures 1 and 5 it can be assumed that the alloy was in the two-liquid region prior to release. The high melt velocities predicted to occur¹¹ in electromagnetic levitated droplets would serve to effectively mix the two liquids. This could account for the fine and uniform distribution of the manganese dendrites (S_1) which initially solidify from the melt. Work to provide a quantitative explanation of the observed microstructure is ongoing.

A novel method of producing and characterizing spheres having uniform phase distributions from otherwise immiscible and difficult to process materials has been demonstrated. As the technique permits significant variation in component materials and their respective volume fractions a number of potential applications can be envisioned. Here unmatched microstructural uniformity can be gained, particularly in combinations of different sizes and materials. Finally, the model developed can be used to guide future studies and fabrications of composite spheres.

CONCLUSIONS

It has been shown that droplets comprising a concentric shell/core (Ag-Ni) or consisting of uniform dispersions (Ag-Mn) can be produced from immiscible, and generally difficult to process, alloy systems. A model has been developed which characterizes and predicts the solidification history of the Ag-Ni composite spheres. A wide range of potential, and novel, applications is suggested in view of the many processing parameters, materials, and dimensions which can be varied.

ACKNOWLEDGMENTS

The authors express their sincere gratitude to Mr. Thomas J. Rathz and the MSFC drop tube team for their effort in facilitating this work. R.N. Grugel gratefully acknowledges the support of NASA grant NAGW-4301.

REFERENCES

1. R.N. Grugel: *Metall. Trans. B*, 1991, vol. 22B, pp. 339.
2. J.B. Andrews, C.J. Briggs, and M.B. Robinson: Materials and Fluid Sciences in Microgravity, Proc. VIIth European Symposium, 1990, ESA SP-295, pp. 121-126.
3. J.B. Andrews, R.A. Merrick, Z.B. Dwyer, A.L. Schmale, C.N. Buckhalt, A.C. Sandlin, and M.B. Robinson: *Materials Science Forum*, 1991, vol. 77, pp. 269-282.
4. Binary Alloy Phase Diagrams, Vol. 1, ed. T.B. Massalski, 1986, ASM.
5. R.N. Grugel, T.A. Lograsso, and A. Hellawell: *Metall. Trans. A.*, 1984, vol. 15A, p. 1003.
6. T.J. Rathz, M.B. Robinson, W.H. Hofmeister, and R.J. Bayuzick: *Rev. Sci. Instrum.*, 1990, vol. 61, pp. 3846-3853.
7. R.N. Grugel and L.N. Brush: "Utilization of a Microgravity Environment to Fabricate Uniformly Composite Spheres From Immiscible Alloy Systems," accepted for publication in the *8th International Symposium on Experimental Methods for Microgravity Materials Science*, March 1996.
8. Thermophysical Properties of Matter, Vol. 1, Thermal Conductivity, IFI/Plenum, New York, 1970.
9. Thermophysical Properties of Matter, Vol. 10, Thermal Diffusivity, IFI/Plenum, New York, 1970.
10. Metals Handbook, Ninth Edition, Volume 2, ASM, 1979.
11. N. El-Kaddah and J. Szekely: *Metall. Trans. B*, 1983, vol. 14B, pp. 401-410.